Seismogeodetic Early Warning System: A Step Forward in Tsunami and Earthquake Warning and Mitigation

Jonatan Glehman [1], Yehuda Bock [1], Barry Hirshorn [1], Allen Nance [1], Jonathan R. Weiss [2], Stuart Weinstein [2] and Dorian Golriz [3]

[1] Institute of Geophysics and Planetary Physics, Scripps Institution of Oceanography, University of California San Diego, La Jolla, CA, USA
[2] Pacific Tsunami Warning Center, National Oceanic and Atmospheric Administration, National Weather Service, Honolulu, HI, USA
[3] Soreq Nuclear Research Center, Yavne, Israel Correspondence to: Jonatan Glehman (jglehman@ucsd.edu)

Group A Poster 017

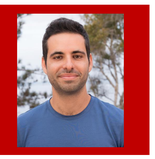

1. Motivation: Seismogeodesy

- Traditionally, tsunami early warning relies on moment magnitude (M_w) and broadband P-wave moment magnitude (M_{wp}) estimates based on regional to teleseismic body waves beyond epicentral distances of ~5°.
- The associated M_w estimation time is inadequate for coastal populations residing closer to big earthquakes (M_w > 8).
- Combining GNSS and collocated strong-motion data:
  - Unclipped broadband velocity and displacement waveforms with a seismic trigger that are sensitive to the entire spectrum of ground motions (seismogeodetic)[1,2].
  - Previously developed approach[3] - Golriz2023 restricted to P-waves propagation suitable for thrust earthquakes but not for other mechanisms.

Extend a physics-based seismogeodetic approach for moment magnitude estimation (M_{wg}) developed for thrust earthquakes to other fault mechanisms

2. Theory
Double-Couple Point Source in a Homogeneous Elastic Medium

Intermediate and far field terms of the radial component of the horizontal motion (h) adopted from [4,5]:

$$u_{hr}(r,t) = \frac{1}{4\pi\rho\alpha^2 r^2} A^{IP} M_0\left(t-\frac{r}{\alpha}\right) + \frac{1}{4\pi\rho\beta^2 r^2} A^{IS} M_0\left(t-\frac{r}{\beta}\right)$$

$$+\frac{1}{4\pi\rho\alpha^3 r} A^{FP} \dot{M}_0\left(t-\frac{r}{\alpha}\right) + \frac{1}{4\pi\rho\beta^3 r} A^{FS} \dot{M}_0\left(t-\frac{r}{\beta}\right),$$

We approximate $\dot{M}_0$ as a backward difference:

$$\dot{M}_0 = \frac{M_0(t) - M_0(t-1)}{dt} \Rightarrow M_0(t) = \left| \frac{u_{hr}(r,t) + \frac{C_{far}}{dt} \cdot M_0(t-1)}{C_{int} + \frac{C_{far}}{dt}} \right|$$

Where:

$$C_{far} = \frac{1}{4\pi\rho\alpha^3 r} A^{FP} + \frac{1}{4\pi\rho\beta^3 r} A^{FS}$$

$$C_{int} = \frac{1}{4\pi\rho\alpha^2 r^2} A^{IP} + \frac{1}{4\pi\rho\beta^2 r^2} A^{IS}$$

$$\mathbf{A^{IP}} = 4\sin 2\theta \cos\phi\, \vec{r} - 2\cos 2\theta \cos\phi\, \vec{\theta}$$

$$\mathbf{A^{IS}} = -3\sin 2\theta \cos\phi\, \vec{r} + 3\cos 2\theta \cos\phi\, \vec{\theta}$$

$$\mathbf{A^{FP}} = \sin 2\theta \cos\phi\, \vec{r}$$

$$\mathbf{A^{FS}} = \cos 2\theta \cos\phi\, \vec{\theta}\,.$$

We assume no radiation pattern corrections for real time implementation:

$$(A^{IP} = A^{IS} = A^{FP} = A^{FS} = 1)$$

3. Data Analysis

Table 1
Earthquakes used in this study
(a) Strike-slip and normal earthquakes

Name/Region	M_w	Fault mechanism	Origin time (UTC)	Longitude (E °)	Latitude (N°)	Depth (km)	Strike/Dip/rake
Ridgecrest, California	7.0	Strike-slip	6 July 2019 03:19:53	-117.600	35.800	8.0	321°/81°/180°
El Mayor-Cucapah, Mexico	7.2	Strike-slip	4 April 2010 22:40:42	-115.295	32.286	10.0	313°/88°/-174°
Pazarcik, Turkey	7.8	Strike-slip	6 February 2023 01:17:34	37.014	37.226	10.0	51°/70°/-4°
Elbistan, Turkey	7.7	Strike-slip	6 February 2023 10:24:48	37.196	38.011	7.4	264°/46°/-9°
Sand Point, Alaska	7.6	Strike-slip	19 October 2020 20:54:38	-159.626	54.602	27.4	350°/49°/176°
Sand Point, Alaska	7.3	Strike-slip	16 July 2025 20:37:39	-160.472	54.549	20.1	344°/57°/157°
Cape Mendocino, California	7.0	Strike-slip	5 December 2024 18:44:21	-125.022	40.374	10.0	280°/83°/-175°
Chiapas, Mexico	8.2	Normal	8 September 2017 04:49:19	-93.899	15.022	47.4	318°/78°/-93°
Rat Islands, Alaska	7.9	Normal	23 June 2014 20:53:09	178.735	51.849	109.0	207°/27°/-13°
(b) Thrust earthquakes studied by Golriz et al. (2023)							
Tokachi-oki, Japan	8.3	Thrust	25 September 2003. 19:50:07	144.079	41.780	42.0	250°/11°/132°
Maule, Chile	8.8	Thrust	27 February 2010 06:34:11	−72.898	−36.122	22.9	19°/18°/116°
Tohoku-Oki, Japan	9.1	Thrust	11 March 2011 05:46:24	142.861	38.104	23.7	203°/10°/88°
Iquique, Chile	8.1	Thrust	01 April 2014 23:46:47	−70.769	−19.610	25.0	355°/15°/106°
Illapel, Chile	8.3	Thrust	16 September 2015 22:54:32	−71.674	−31.573	22.4	007°/19°/109°
Kilauea, Hawaii	6.9	Thrust	04 May 2018 22:32:54	−155.000	19.318	5.8	238°/19°/106°
Simeonof, Alaska	7.8	Thrust	22 July 2020 06:12:44	−158.522	55.030	28.0	243°/17°/92°
Chignik, Alaska	8.2	Thrust	29 July 2021 06:15:49	−157.888	55.364	35.0	238°/10°/88°

3. Results

I. New Method with and without Radiation Pattern (RP) Correction vs. Previous Method (Golriz2023)

→ M_{wg} with an accuracy of ±0.2 units, for most of the strike-slip events, without RP corrections.
→ RP corrections offer substantial benefits for normal and thrust faulting events. Golriz2023 performs better.

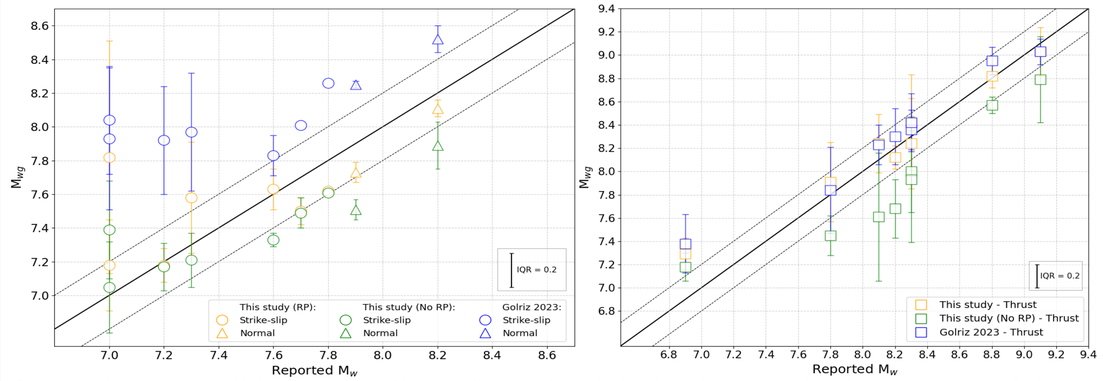

Seismogeodetic magnitude (M_{wg}) estimates for (left): strike-slip, normal, and (right): thrust fault earthquakes. Marker shapes denote fault type (strike-slip = circles, normal = triangles, thrust = squares). Colors indicate methods. The solid line marks the 1:1 relation with reported Mw, and dashed lines show ±0.2 IQR.

II. Spatial and Temporal Performance – No RP Corrections Suitable for Real Time Implementation

→Larger discrepancies observed for events with sparse near−source coverage/complex rupture behavior.
→ Most events stabilize within 100–150 seconds despite having a low coverage (≤ 5 stations).

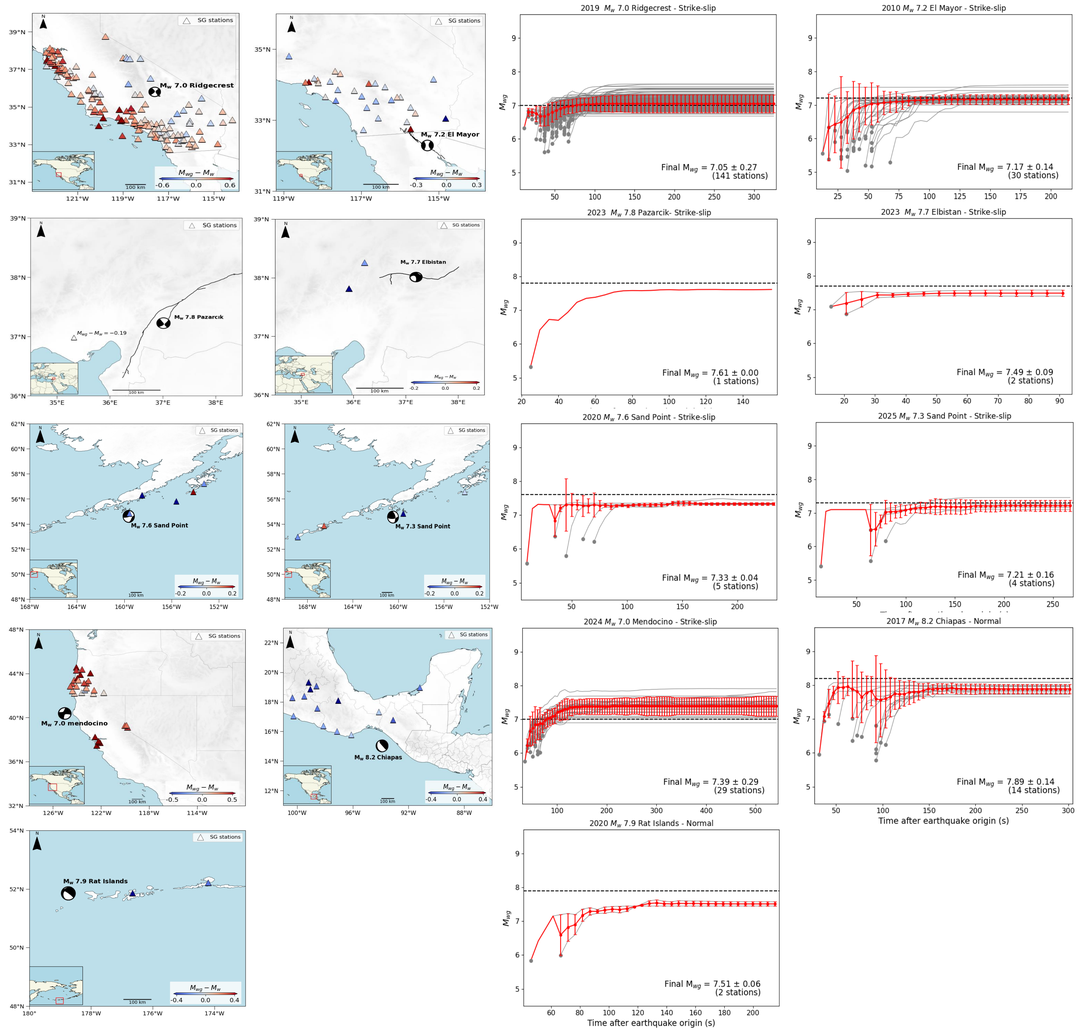

Seismogeodetic magnitude (M_{wg}) estimates without RP corrections for seven strike-slip and two normal earthquakes (Table). (Left): Station-level estimates, with red indicating overestimates and blue underestimates. (Right): Time evolution of event magnitudes; gray = individual stations, red = event medians (±IQR), black dashed lines = GCMT magnitudes.

III. Stand-Alone GNSS with an Interpolated Coseismic Window Supplement the Collocated Stations

→ M_{wg} within ±0.2 units of the collocated estimates in most cases
→ The estimates tend to be slightly lower than collocated station-based

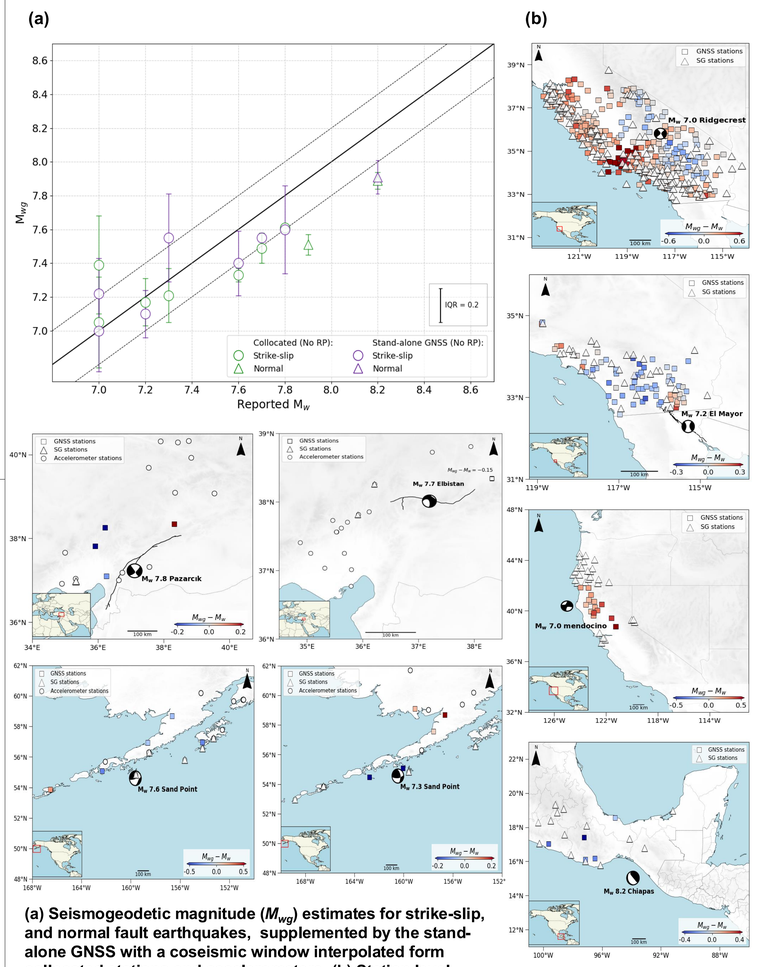

(a) Seismogeodetic magnitude (M_{wg}) estimates for strike-slip, and normal fault earthquakes, supplemented by the stand-alone GNSS with a coseismic window interpolated form collocated stations and accelerometers. (b) Station-level estimates, with red indicating overestimates and blue underestimates.

4. Conclusion - Unified Approach to Earthquake and Tsunami Early Warning

- New algorithm performs well for strike-slip events without RP corrections.
- Largely underestimates normal and thrust earthquakes if RP corrections not applied.
- Golriz2023 suits thrust events but overestimates strike-slip/normal.
- Obtaining radiation patterns in real time is challenging, Golriz2023 preferred for non-strike-slip earthquakes.
- An integrated workflow for rapid magnitude estimation, which leverages tectonic context (Slab2 geometry) to inform model selection.
- Offers a viable and efficient solution for operational use, in both earthquake and tsunami early warning systems.

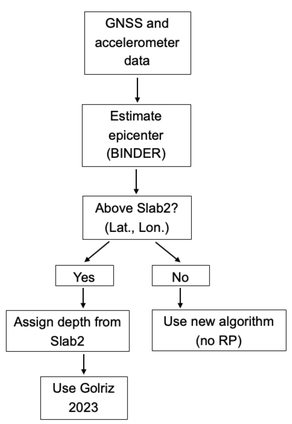

References
[1] *Smyth & Wu 2007; Mechanical Systems and Signal Processing* , *21*(2), 706-723
[2] Bock et al 2011; BSSA, *101*(6), 2904-2925
[3] *Golriz et al 2023; JGR, 128*(1), e2022JB025555
[4] Madariaga et al. 2019; *Pure and Applied Geophysics*, *176*(3), 983-1001
[5] Aki and Richards (2002); Quantitative seismology.